

Bond resistance of prestressed CFRP strips attached to concrete by using EBR and EBROG strengthening methods

Niloufar Moshiri^{a,b}, Christoph Czaderski^{b,*}, Davood Mostofinejad^a, Masoud Motavalli^{b,c}

^a Isfahan University of Technology (IUT), Department of Civil Engineering, Isfahan, Iran

^b Swiss Federal Laboratories for Materials Science and Technology (Empa), Structural Engineering Research Laboratory, Dübendorf, Switzerland

^c University of Tehran, College of Engineering, Faculty of Civil Engineering Tehran, Iran

HIGHLIGHTS

- Concrete blocks were strengthened by prestressed CFRP composites.
- Bond resistance was determined through prestress force-release tests.
- EBROG method increased the bond resistance with a factor of 2.4.
- EBROG method increased the fracture energy by introducing crack growth in a large failure plane.

ARTICLE INFO

Article history:

Received 11 March 2020

Received in revised form 1 October 2020

Accepted 4 October 2020

Available online 24 October 2020

Keywords:

Prestressed CFRP

Prestress force-release test

Externally bonded reinforcement on grooves

EBROG

3D DIC

EBR

Concrete strengthening

ABSTRACT

Strengthening reinforced concrete (RC) beams and slabs with prestressed carbon fiber-reinforced polymer (CFRP) composites is of high interest since the FRP material can be used more efficiently. Developing a non-mechanical prestressed strengthening system entails evaluating the bond resistance of prestressed FRP to the substrate. To increase the bond resistance of prestressed CFRP strips to the concrete substrate, a new method called externally bonded reinforcement on grooves (EBROG) was investigated and compared with the conventional externally bonded reinforcement (EBR) method. For this purpose, prestress force-release tests were performed to study the bond behavior of prestressed FRP to concrete. In-plane and out-of-plane deformations were measured through a three-dimensional digital image correlation (3D DIC) system. All the tests were carried out at Empa Structural Engineering Laboratory in Dübendorf, Switzerland.

Experimental results showed that the average bond resistances of EBR and EBROG joints in prestress force-release experiments were 34.4 and 81.4 kN, respectively; indicating an increased bond resistance for the EBROG method with a factor of 2.4. By using the EBROG method, the failure plane incorporated massive crack development in concrete bulk and therefore, the fracture energy and bond resistance of prestressed joints increased significantly. Besides, it was shown that prestressed joints experienced large out-of-plane deformations, emphasizing the fact the bond behavior of prestressed FRP to concrete should be treated as a mixed shear/tension fracture mode in the future studies.

© 2020 The Authors. Published by Elsevier Ltd. This is an open access article under the CC BY-NC-ND license (<http://creativecommons.org/licenses/by-nc-nd/4.0/>).

1. Introduction

The application of fiber-reinforced polymer (FRP) composites in strengthening reinforced concrete structures has increased over the past decades. Their superior properties, such as being lightweight, high-strength, corrosion-resistant, and easy to apply, pave the road for their usage [1]. However, premature debonding of FRP from the concrete substrate is a drawback, as it reduces the

strengthening efficiency [2,3]. Low strain levels compared to the ultimate FRP strain can be developed before debonding. Therefore, the full capacity of the material is not utilized. To overcome this issue, prestressing FRP was proposed and put into practice. Higher strain values are developed in the composite, which implicates better efficiency of the FRP high-tensile strength. By decreasing the tensile stress in internal steel reinforcements, prestressed FRP can help to increase the fatigue strength of FRP-strengthened beams. Besides, the prestressed FRP application enhances the serviceability state by increasing the cracking load and decreasing the crack width and deflection of the strengthened beam [4–9].

* Corresponding author.

E-mail address: christoph.czaderski@empa.ch (C. Czaderski).

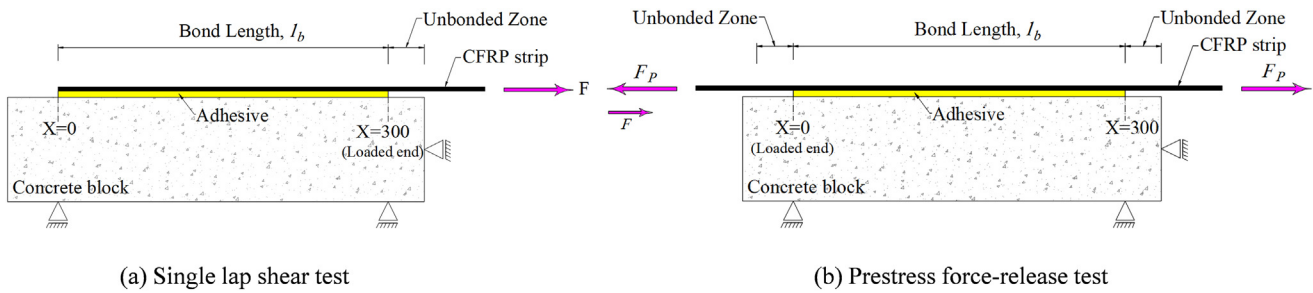


Fig. 1. Schematic test types (dimensions are in mm).

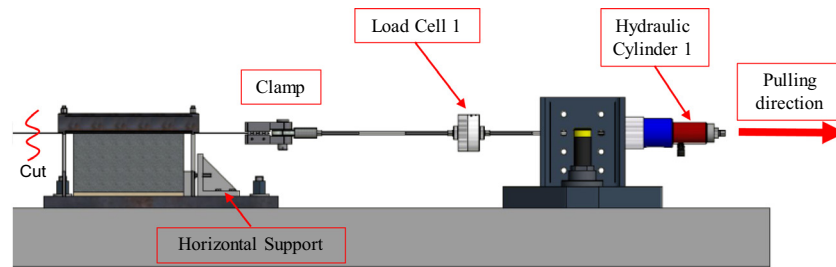


Fig. 2. Schematic single-lap shear test setup.

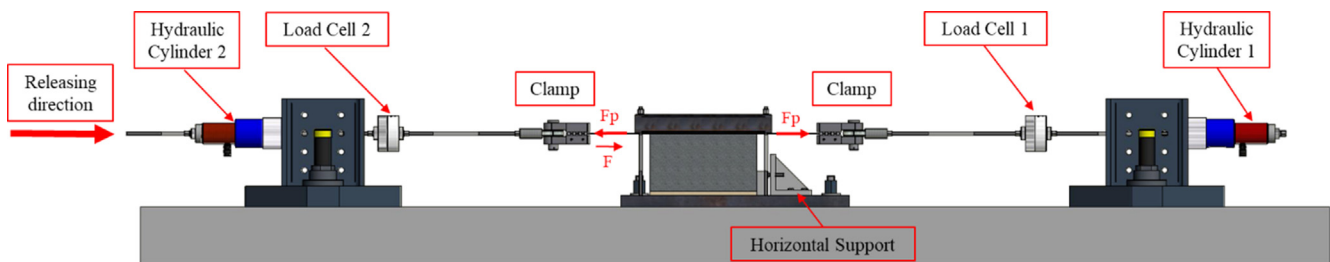


Fig. 3. Schematic prestress force-release test setup.

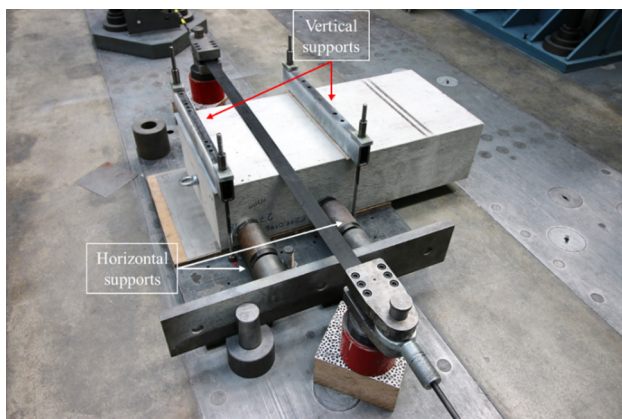


Fig. 4. Fixation and supports of the test specimen.

A major concern regarding the prestressed FRP is to secure the anchoring of the strip so that the prestressing force can transfer from FRP to the concrete. Mechanical anchorage is generally used for this purpose. Different mechanical systems were proposed and tested [10–14]. Mechanical anchors can prevent end debonding and end cover separation [15]. A nonmechanical anchorage system called gradient anchorage was introduced at Empa [16–18].

For this non-mechanical anchorage, no plates or bolts are remaining. In this system, after applying the FRP strip on the substrate and prestressing it, the epoxy adhesive between the strip and substrate undergoes accelerated curing over several sectors. In each step, part of the prestressing force is released, and the force is transferred to the concrete substrate. Following this procedure, no prestressing force exists at the strip end and, therefore, no mechanical anchorage is needed. The force that can be released in each sector and the sector's length were investigated by Czaderski et al. through a prestress force-release test [16,17,19]. In this test, the FRP strip is first applied on the substrate and prestressed up to the determined value. The prestressing force is kept constant over several days until the epoxy adhesive is cured. Then, the force is gradually released until a failure happens in the FRP-to-concrete bonded joint. A similar concept, i.e. prestress-force releasing through several steps were also studied by He et al. [20]. It was demonstrated that in a prestress force-release test, failure mode I is dominant, while the prevailing mode in a lap shear test is mode II. Therefore, out-of-plane deformations play an important role in describing the bond behavior of prestressed FRP [16].

When FRP is prestressed, higher strains are developed in the FRP before failure, and therefore, it can be used more efficiently. A great interest in strengthening RC beams and slabs with prestressed CFRP composites would then come up. If metallic end anchorages can be removed, the strengthening procedure is more

likely to be cost-efficient, easy to apply, and resistant to corrosion; and thus, more interesting to engineers. In another research work of the authors, RC beams and slabs were strengthened by prestressed CFRP without using any metallic end anchorages [9,21]. In these studies, the EBROG method was used to postpone the debonding of prestressed FRP from the concrete substrate. Determining the ultimate bond resistance of prestressed FRP to concrete, when the EBROG method is used, is necessary to propose design schemes. A prestress force-release test is aimed at determining the bond resistance of prestressed FRP strip to concrete while having no mechanical metallic anchorages.

The externally bonded reinforcement on grooves (EBROG) method was introduced as a substitute for the EBR method to improve the structural behavior of FRP-strengthened members in

different applications [22–28]. This method was first developed at Isfahan University of Technology (IUT) to improve the flexural capacity of FRP-strengthened concrete beams [22]. Enhancing the bond behavior of unstressed FRP to concrete by using the EBROG method was well approved through previous research studies [29–35]. It was demonstrated that by using the EBROG method, the bond resistance increased significantly. Besides, by using the EBROG method in strengthening beams, FRP debonding was postponed or in some cases eliminated [22,23]. The effect of EBROG on compression and the bending capacity of columns, shear capacity of beams, and beam-to-column joints was confirmed as well [25–27,36]. Considering the advantages of prestressed FRP, there is high motivation to use EBROG in strengthening with prestressed FRP.

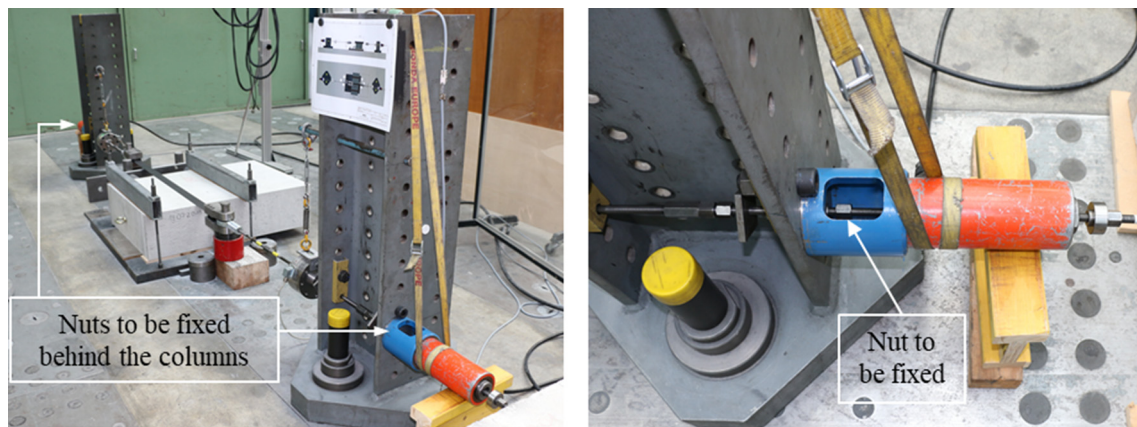


Fig. 5. Position of the nuts behind the columns which were fixed to keep the prestressing force constant in the strip.

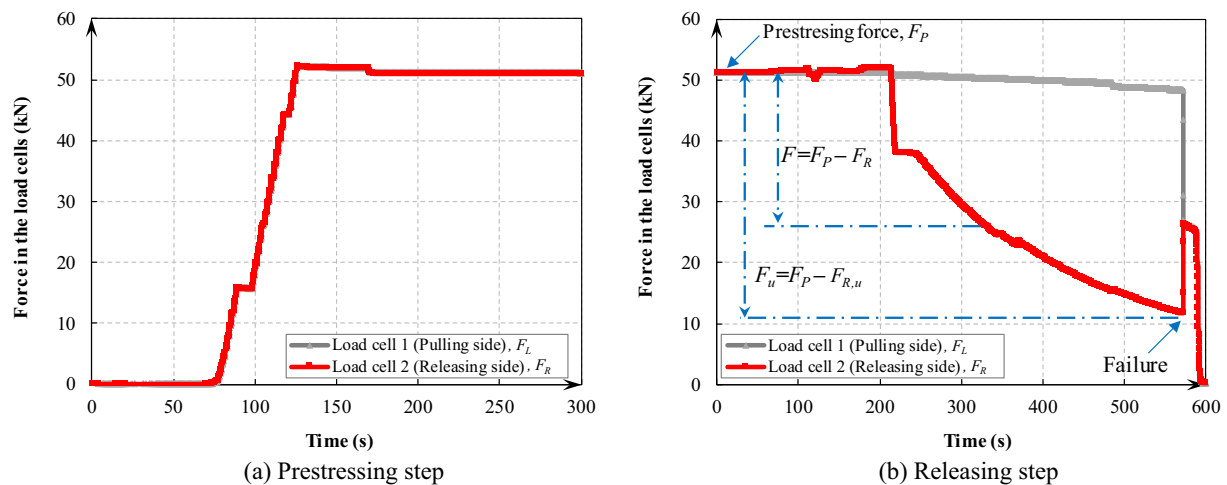


Fig. 6. Force in the two load cells and calculation of the bond resistance for a release test (diagrams correspond to specimen “R-EBR-1”).

Table 1
Test layout.

Specimen label	Strengthening method	Test type	Number of longitudinal grooves	Groove dimensions	
				Width, b_g (mm)	Depth, h_g (mm)
L-EBR-1	EBR	Lap shear	–	–	–
L-EBR-2	EBR	Lap shear	–	–	–
L-EBROG-1	EBROG	Lap shear	2	10	10
L-EBROG-2	EBROG	Lap shear	2	10	10
R-EBR – 1	EBR	Prestress force-release	–	–	–
R-EBR-2	EBR	Prestress force-release	–	–	–
R-EBROG-1	EBROG	Prestress force-release	2	10	10
R-EBROG-2	EBROG	Prestress force-release	2	10	10

In this study, the effect of the EBROG method on the bond behavior of prestressed FRP-to-concrete was investigated for the first time. By evaluating the bond resistance in the EBROG method, it can be used in design recommendations for the flexural strengthening of RC beams with prestressed CFRP composites. Four prestress force-release tests were carried out, as well as four single-lap shear tests for the sake of comparison. Concrete blocks were strengthened via EBR or EBROG to compare these two methods. Since out-of-plane deformations dominate the behavior of the prestressed FRP, a full-field three-dimensional digital image correlation (3D DIC) system was utilized to measure the displacements in all tests. The bond resistance, failure mode, and displacement field were investigated in detail. This study is a pioneer in using the EBROG method to anchor prestressed FRP strips onto concrete. Since there would be no permanent steel plates or dowels, the EBROG anchorage to transfer prestressing force at strip ends provides an easy, cost-efficient, and corrosion-resistant anchorage system. Potential applications for prestressed FRP strengthening anchored through the EBROG method, include strengthening of slabs, RC beams, or bridge decks. It is worth mentioning that this study was among the pioneers to use the EBROG method for anchoring prestressed FRP to the concrete substrate.

It is worth mentioning that the specimens in this study were briefly introduced in two conference papers during the SMAR 2019 conference, Potsdam, Berlin, Germany [37,38].

2. Experiments

2.1. Test setup

Two test types were conducted in this research: single-lap shear and prestress force-releasing test. Test types are schematically illustrated in Fig. 1 and are depicted in detail in Fig. 2 and in Fig. 3.

The first tests were single-lap shear tests in which the bond behavior of the unstressed FRP (without any prestressing force) was studied. The single-lap shear test setup is depicted in Fig. 2. In the lap shear test, the tensile force was applied on one end of the FRP strip in a load-control mode. It was performed by hydraulic cylinder No. 1 in Fig. 2 to the right side of the picture and was measured using load cell 1. In the lap shear tests, the concrete block was initially fixed on the support. The support included a thick metal plate that was tightly fixed to the strong floor. Two beam-like supports were then fastened on the block to prevent its vertical displacement (see Fig. 4). Block movement in the horizontal direction and parallel to the strip was restrained by two horizontal constraints (see Fig. 4). After several days of curing, the specimen was made ready for the lap shear test. Eventually, the force was applied on the right side in Fig. 2 by manually increasing the oil pressure in the hydraulic jack. The maximum force carried by the FRP-to-concrete bonded joint was called bond resistance. Force was measured by a 150 kN load cell with a frequency of 5 Hz.

Table 2
Concrete mix design proportions.

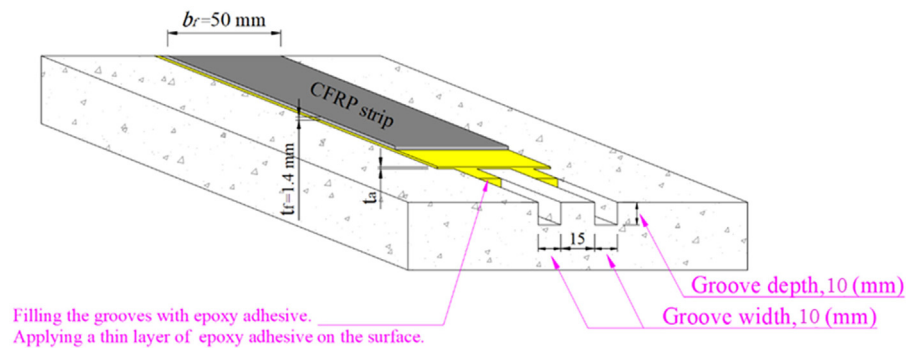
Constituent	Fine aggregate(0–4 mm)	Coarse aggregate(4–8 mm)	Coarse aggregate(8–16 mm)	Coarse aggregate(16–32 mm)	Cement	Water
Amount (kg/m ³)	751.4	276.8	316.4	632.7	275	168



Fig. 7. Clamping the FRP strip in both ends.

Full-field displacement measurements were carried out via the 3D DIC system. A further description about the DIC system is discussed in section 2.5.

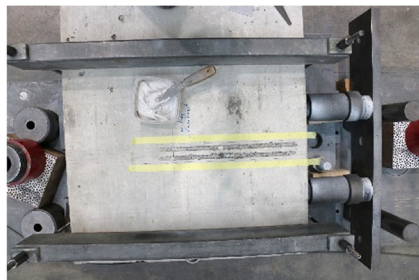
The second test type was a prestress force-release test in which the bond behavior of the prestressed FRP was studied. The release test setup is shown in Fig. 3. The test consisted of three main steps:



(a) Schematic view of the longitudinal grooves, adhesive layer and CFRP strip



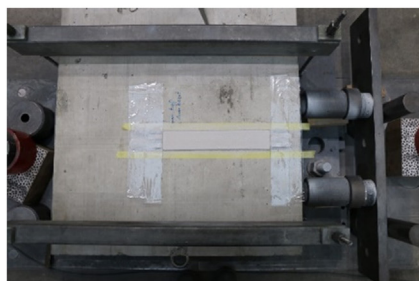
(b) Cutting the grooves by means of a circular saw



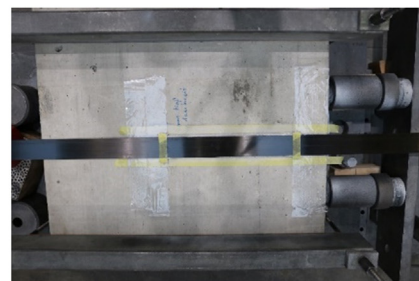
(c) Longitudinal grooves cut into the concrete surface



(d) Filling the grooves with epoxy adhesive



(e) Applying a layer of adhesive on the surface



(f) Bonding CFRP strip

Fig. 8. EBROG method.

- 1) bonding the strip onto the concrete substrate over 300 mm bond length and initially prestressing the strip,
- 2) keeping the prestressing force constant over 6–7 days until complete adhesive curing, and
- 3) finally releasing the force on one strip end until failure.

Supports and fixation of the block in the prestress force-release test were the same as those of the lap shear test. Bonding the strip on the block followed by prestressing it up to the determined prestress level was the next step. During bonding and prestressing the strip, no interfacial stress existed between the strip and concrete, since the adhesive was completely uncured and fluid. For the period of curing, the prestressing force was kept constant by fixing the nuts behind the columns (see Fig. 5). This way, the oil pressure in the hydraulic jacks can be released completely while the prestressing force is continuous in the steel rods and in the strip. After complete epoxy curing, the specimen was made ready for the prestress force-release test. To do so, the oil pressure in hydraulic jack number 2 was increased so that the nut was loosened and opened completely. Eventually, the test was performed by manually decreasing the oil pressure in hydraulic jack 2 in load-control mode (F_R = existing force in the load cell 2; F = force changes in the load cell 2 or the force that is released). The difference between the existing force in the strip at failure ($F_{R,u}$) and the prestressing force immediately before the start of releasing (F_P), was determined as the bond resistance (bond resistance = $F_u = F_P - F_{R,u}$). Forces at both strip unbonded lengths were measured by two 150 kN load cells with a frequency of 5 Hz for prestressing/releasing steps, and with a frequency of 2 Hz for the curing step. The force in two of the load cells and the determined bond resistance of a release test are illustrated in Fig. 6, for specimen “R-EBR-1”, as an example. Full-field displacement measurements were carried out via the 3D DIC system as well.

The criteria for selecting the initial prestressing force was that the failure during the release must be reached. In other words, the initial prestressing level was selected so high to make sure that during the test, when the released force was being carried by the joint, the capacity of the joint was reached and failure occurred. It is obvious that the so-called high prestressing level varies from specimen to specimen and depends on the specimen configuration and the strengthening method. It is worth mentioning that another possible force configuration is the low prestressing level. In this case, failure would not happen during release, and an additional tensile force should be applied on the other strip end to obtain failure. This type of test is called the mixed lap shear/release test [16].

2.2. Test layout

A total of eight tests were performed to evaluate the bond behavior of unstressed and prestressed FRP to concrete. The test layout is demonstrated in Table 1. The specimens' labels start with the capital letter “L” for lap shear tests or “R” for prestress force-release tests (can be called release test for simplicity), followed by the strengthening method and number 1 or 2 for the repetition of a test. For example, “R-EBROG-1” denotes the first release test on a specimen strengthened by using the EBROG method.

2.3. Material properties

Concrete blocks with a maximum aggregate size of 32 mm and the mix design according to Table 2 were cast. Using three standard concrete cubes of 150 mm, the cylinder concrete compressive strength for each specimen was determined for the lap shear/release testing date. Concrete blocks dimensions were 473 mm in length (parallel to the steel rods and the strip longitudinal direction), 1000 mm in width, and 250 mm in height.

Unidirectional carbon-FRP strips with 1.4 mm thickness and 50 mm width, which were cut into pieces of 1500 mm length, were used for strengthening the concrete blocks. The CFRP strips, of type S&P C-Laminates CFK 150/2000–50/1.4, had a fiber volume fraction of 68%, a nominal tensile strength of 2800 MPa [39]. The elastic modulus of the strips was measured as 160 GPa. The FRP strip was bonded onto the concrete substrate over a 300 mm bond length in the middle of the block, meaning that 86.5 mm was left unbonded on each side of the block. A two-component epoxy adhesive was used to bond the FRP strip on the surface and to fill the grooves. The S&P 220 epoxy adhesive had an elastic modulus of 9.32 GPa, an ultimate tensile strength of 18.9 MPa, and an ultimate tensile strain of 0.24% [40].

2.4. Specimen preparation

At first, the concrete block was fixed on the test setup. The FRP strip was placed in two end clamps and tightly fixed with 6 bolts (each with 125 kN.m) in each clamp (Fig. 7). Strengthening the concrete block with FRP strip was performed with two different methods of EBR and EBROG. The bond length was 300 mm for all specimens. The procedure for each method is as follows:

EBR method:

- 1) Removing a weak thin layer of the concrete surface by grinding the surface with a disk grinder.
- 2) Cleaning the dust on the substrate with compressed air.
- 3) Applying a layer of epoxy adhesive on the surface.
- 4) Cleaning the FRP strip with S&P cleaner and bonding the strip onto the concrete with an epoxy adhesive.

EBROG method:

- 1) Cutting two longitudinal grooves into the concrete substrate longer than the determined bond length and with a free distance of 15 mm from each other by using a circular saw. The groove cross-section was 10 mm depth (h_g) and 10 mm width (b_g). In contrast to the EBR method, the weak thin layer of concrete was not ground in EBROG.
- 2) Cleaning the dust on the substrate and inside the grooves with compressed air.
- 3) Filling the grooves with epoxy, followed by applying a thin layer of epoxy on the specimen's surface.
- 4) Cleaning the FRP strip with S&P cleaner and bonding the strip onto the specimen's surface by using an S&P220 epoxy adhesive

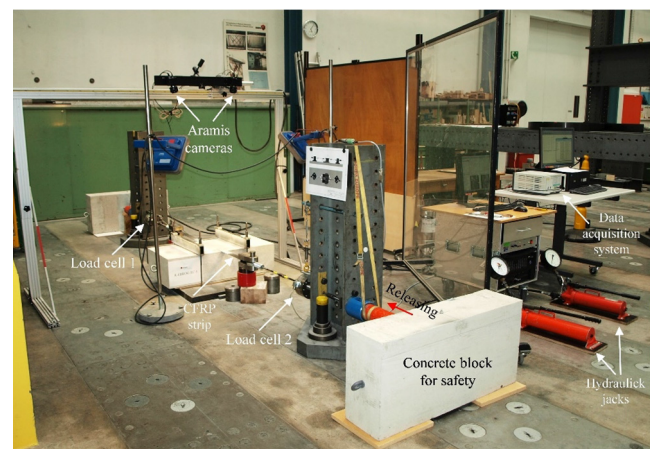


Fig. 9. DIC measurement system.

The successive steps in the EBROG method are shown in Fig. 8. Based on the authors' previous study [31], the 10×10 mm groove cross-section resulted in the highest improvement in bond resistance of unstressed joints, and therefore, this dimension was selected in this study to compare the bond behavior of unstressed and prestressed joints.

2.5. Three-dimensional digital image correlation (DIC)

Full-field deformation measurement was achieved by using a 3D digital image correlation (DIC) system, commercially known as Aramis (GOM GmbH, Braunschweig, Germany) [41]. To provide an appropriate texture for image processing, a white and black pattern was produced on the specimen's surface by using a white color brush and an airbrush for black spots. 3D deformations, i.e., in-plane and out-of-plane displacements on the strip and on the surrounding concrete were evaluated by using DIC monitoring from the top. Two digital cameras with 4-megapixel resolutions were mounted on an aluminum frame with the focus on a 350×350 mm area, which is called the volume size in the software. Consecutive images were taken from the specimen's face during the test and were called stages. Tracking successive images and comparing them with the first image taken in stage 0 just before the start of the test revealed the deformations/strain field. Failure mode was well understood by interpreting the crack propagation in Aramis software. Based on the software's manual, the accuracy of displacements measurement for in-plane and out-of-plane deformations is in the range of 0.01–0.1 pixel and 0.1–1.0 pixel, respectively. Considering the 350×350 vol size, which was monitored by a 2000×2000 pixels (4 megapixels) camera, the accuracy would be between 0.002 and 0.018 mm for in-plane deformations and 0.018–0.175 mm for out-of-plane deformations. Validation of the DIC system was demonstrated in previous studies [40]. It is worth mentioning that the subsets of 15×15 pixel with 13 pixel transition were generated in all experiments. The test setup for the release experiments and the DIC measurement system are shown in Fig. 9.

3. Results and discussion

3.1. Bond resistance

Experimental test results are reported in Table 3. The maximum force carried by the FRP-to-concrete bonded joint is called the

bond resistance. It was the maximum pulling force for the lap shear test. In the release test, the maximum force that was resisted by the bond was the difference between the prestressing force and the force in the releasing side of the strip at the ultimate load (Fig. 6). It is worth mentioning that the initial prestressing force slightly changed during the curing time probably due to changes in temperature. Thus, the prestressing force immediately before the start of the releasing test was considered in calculating the bond resistance. As mentioned before, forces in both the lap shear and in the releasing tests were measured by load cells, and these measurements were recorded by the DIC software as well. The frequency of measurements for load cells was 5 Hz, while it was 1 Hz for DIC. This means that successive images were taken every 1 s in the DIC measurement system (they are called stages). For the sake of conformity, the final stage of DIC was selected to calculate the force, as it was also used for calculating the displacements. Therefore, the maximum force at the final stage of DIC was selected as the bond resistance. However, it might be slightly different from that of the ultimate load in load cell measurements.

The bond resistances for all experiments are presented in Fig. 10. It can be observed that the bond resistance for two lap shear tests of the EBR method was 26.88 and 31.79 kN; it was 48.91 and 49.58 kN for lap shear tests of the EBROG method. This means that the bond resistance for EBROG was approximately 68% higher than that of EBR. Such significant improvement for EBROG joints was approved in previous studies as well (it is obvious that

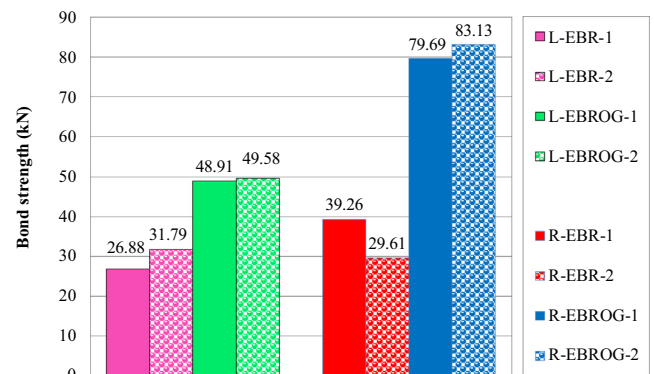


Fig. 10. Bond resistances.

Table 3

Test results.

Specimen label	f'_c (MPa)	Prestressing force* (kN)	Prestressing level** (kN)	Bond resistance (kN)	Initiation of debonding				Final stage			
					Stage No.	Carried force† (kN)	s_f (mm)	r_f (mm)	Stage No.	Carried force† (kN)	s_f (mm)	r_f (mm)
L-EBR-1	41.8	–	–	26.88	30	24.39	0.147	0.342	34	26.88	0.316	0.589
L-EBR-2	43.2	–	–	31.79	60	31.79	0.198	0.078	62	31.42	0.423	0.824
L-EBROG-1	41.8	–	–	48.91	76	48.63	0.205	0.188	77	48.69	0.258	0.375
L-EBROG-2	43.2	–	–	49.58	66	49.37	0.213	0.033	69	49.58	0.530	0.471
R-EBR-1	41.8	51.86	26%	39.26	263	26.45	0.159	0.299	436	39.26	0.712	1.838
R-EBR-2	41.8	48.80	25%	29.61	225	22.00	0.135	0.324	276	29.61	0.548	1.804
R-EBROG-1	41.8	100.05	51%	79.69	578	79.69	1.104	5.576	602	79.69	1.590	8.694
R-EBROG-2	41.8	101.88	52%	83.13	636	83.06	1.615	10.038	637	83.13	1.676	10.573

† The force which is carried by the bonded joint up to this stage.

Comments:

f'_c = Cylindrical concrete compressive strength

s_f and r_f are the strip slip and separation, respectively, measured at the loaded end. (Loaded end is the point on the central strip axis at $X = 300$ mm for lap shear tests where the tensile pulling force is applied, and it is at $X = 0$ mm for prestress force-release tests where the initial prestressing force is released.)

* Immediately before the start of the prestress release test.

** Concerning the ultimate capacity of the CFRP strip (196 kN).

the increased percentage depends on the material properties, fiber thickness, groove dimensions, concrete compressive strength, and other parameters [28,31,32]). Besides, an even larger increase in the bond resistance of prestress force-release tests was achieved for the EBROG method compared to the EBR method (Fig. 10). While two repetitions of the EBR release tests ("R-EBR-1" and "R-EBR-2") showed a bond resistance of 39.26 and 29.61 kN, release tests, which were strengthened via EBROG, achieved a bond resistance almost twice the maximum of EBR tests. Specimens "R-EBROG-1" and "R-EBROG-2" had bond resistances equal to 79.69 and 83.13 kN, respectively.

It is worth mentioning that the prestressing force for specimens was selected high enough that during releasing of the force, complete failure happens (see Fig. 6b). Therefore, EBROG joints were prestressed up to a higher prestressing force, compared to EBR joints.

3.2. Failure mode

Failure modes for the lap shear and release experiments are illustrated in Figs. 11 and 12, respectively. As expected, in lap shear tests that were strengthened with the EBR method, the FRP strip together with a thin layer of concrete debonded from the substrate. In lap shear tests that were strengthened with the EBROG method, however, debonding of the FRP strip occurred in the adhesive layer, which means that the concrete substrate was no longer the weakest constituent in the FRP/adhesive/concrete system. On the other hand, the longitudinal grooves and the concrete substrate, as a package, were a strong support for carrying the load from FRP to

the substrate. Cohesion failure mode (failure in the adhesive layer) for the EBROG joints was previously reported when EBROG was used to attach the unstressed precured FRP strips [31].

Failure mode in the release tests of "R-EBR-1" and "R-EBR-2" occurred as debonding in a thin layer of concrete just beneath the strip. Only a small lateral spreading occurred in these two specimens. Very different was the failure mode of the prestressed EBROG joints, in which the FRP debonded together with a very huge concrete volume. In specimens "R-EBROG-1" and "R-EBROG-2," cracks started much before the maximum bond resistance reached. During the release, the cracks propagated not just beneath the strip, but they also developed laterally to the strip borders and in the surrounding concrete. Moreover, debonding cracks developed deep in the concrete, thus representing strong out-of-plane movements. A large area of the concrete substrate was, therefore, cracked by releasing the force, which indicated that high fracture energy was released. High bond resistance for EBROG joints is, therefore, attributed to high fracture energy.

3.3. Load-relative displacement behavior

By using a 3D DIC system, longitudinal and out-of-plane deformations were assessed for all experiments. To better interpret the global behavior, in this chapter, FRP strip displacements were considered throughout several sections (Sections 0, 1, and 2 in Fig. 13). The coordinate system and locations of the sections are shown in Fig. 13. The bond length was from $X = 0$ to $X = 300$ mm. Section 0 is a longitudinal section in the middle of the strip, and Sections 1

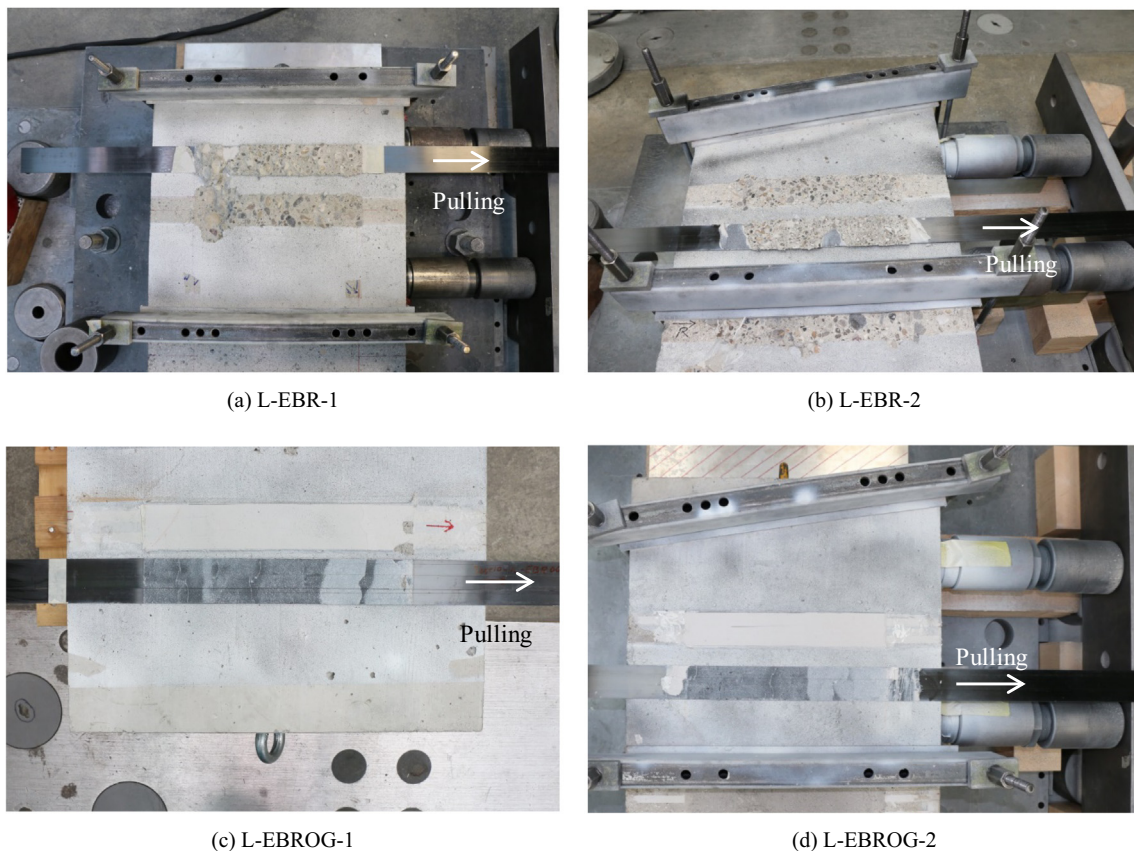


Fig. 11. Failure modes of lap shear experiments.

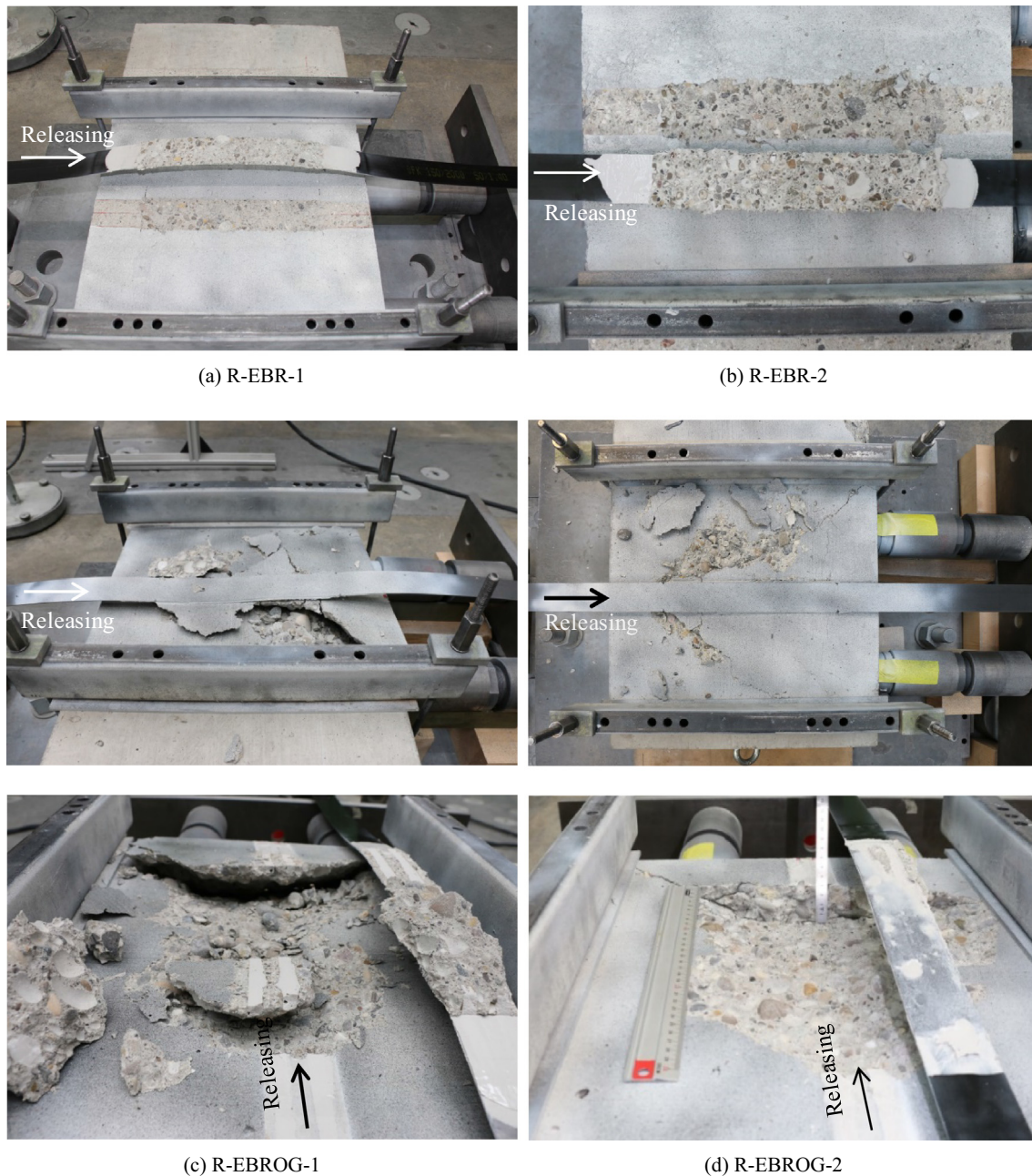


Fig. 12. Failure modes of prestress force-release experiments.

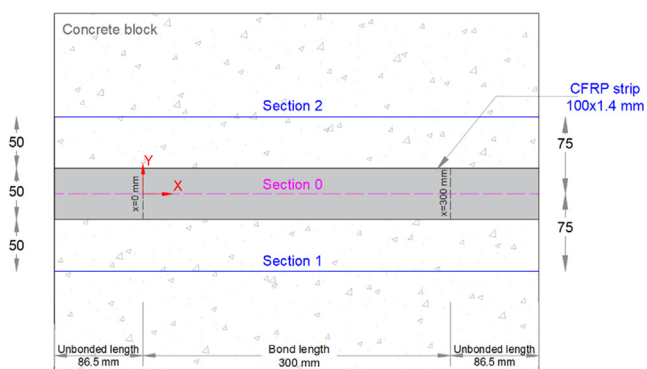
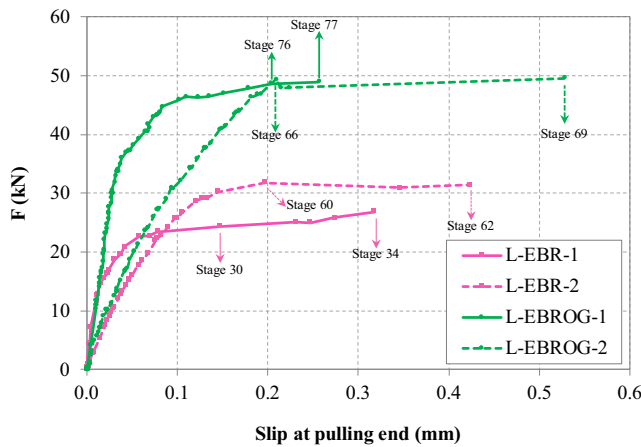


Fig. 13. Coordinate system and sections definitions (dimensions are in mm).

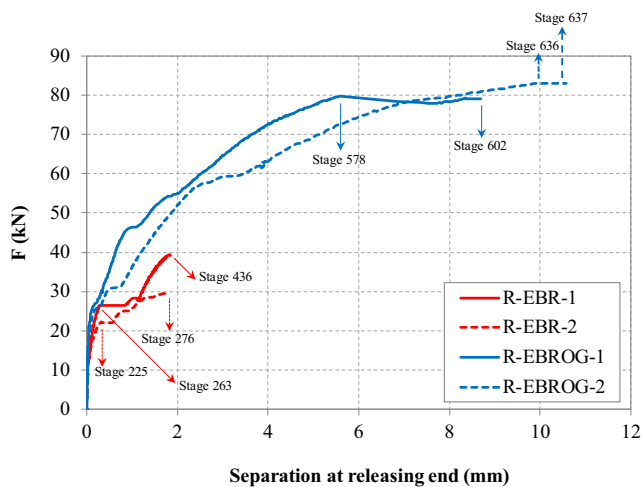
and 2 are two longitudinal sections on the concrete, with 75 mm spacing to the strip centerline. Slip, i.e., the relative longitudinal displacement of the strip with respect to the concrete substrate, s_f , was determined by subtracting the average of the longitudinal displacements of Sections 1 and 2 from the longitudinal displacements of Section 0.

The general behavior of specimens is demonstrated in Fig. 14 in terms of the load-slip and load-separation diagrams for the point of “loaded end” on the strip. The loaded end is the pulling end for lap shear tests ($X = 300$ mm) and the releasing end for release tests ($X = 0$ mm). The force of the prestress force-releasing test was converted for comparison reasons (i.e., the force increases instead of reduces).

Load versus slip at the loaded end is depicted in Fig. 14 (a) for unstressed joints. Bilinear behavior can be observed for the lap



(a) Load-slip of unstressed joints



(b) Load-separation of prestressed joints

Fig. 14. Load-deformation behavior of tested specimens.

shear tests, whether the EBR or the EBROG method was used. However, for the EBROG method, higher force and slip values were achieved at the final stage, as well as at the stage of initiation of debonding.

It was discussed by Czaderski that out-of-plane deformations dominate the bond behavior of prestressed FRP [16]. Relative out-of-plane deformation of the strip with respect to the concrete substrate was called separation, r_f . The load-separation behavior of the prestressed joints at the loaded end ($X = 0$ mm) is represented in Fig. 14 (b). For this purpose, the average out-of-plane deformation of concrete in sections 1 and 2 was deducted from that of the strip. It can be observed from the figure that a tremendous increase in the force and separation was achieved for prestressed EBROG joints, compared to those of the prestressed EBR joints. In other words, EBR joints that were strengthened by the prestressed FRP, revealed a maximum separation equal to 1.82 mm on average, while the prestressed EBROG joints reached to a separation of 9.63 mm on average. Therefore, as the deformation increased, the EBROG joint could resist and transfer high forces to the substrate before failure.

Using the EBR or EBROG methods led to different behaviors of the prestressed joints (Fig. 14 b). In other words, several plateaus were experienced in the EBR joints, while the EBROG joints exhibited an increasing trend up to the maximum. When the EBR

method was used to attach the prestressed FRP to concrete, several horizontal plateaus were observed. It means that separation increased considerably without an increase in the carried load. This phenomenon can be called local debonding, which indicates that a further increase in the load is possible. This can be attributed to a crack development under the strip. Czaderski demonstrated that in a prestress force-release test in the EBR method, especially when the bond length is short, the cracks were generated and developed inclined to the concrete depth [16]. An aggregate interlock can be another parameter that affected this load increase after local debonding.

3.4. Deformations

Using the 3D DIC system, the evolution of in-plane and out-of-plane deformations were well described during the experiment. Slip and separation evolution along the strip are explained in the following sections.

3.4.1. Unstressed FRP

Slip (s_f) of the central strip axis in X direction during successive loading stages is illustrated in Fig. 15 for lap shear tests. In lap shear tests, the tensile load was applied on the loaded end at $X = 300$ mm. Thus, the slip propagated from $X = 300$ mm to the unloaded end at $X = 0$ mm. By increasing the load, a longer bond length experienced slip and was active in transferring the load. In lap shear tests, the active length at the initiation of the debonding stage is called the effective bond length. The initiation of debonding is the stage that corresponds to a significant increase in the slip without a considerable increase in the load. To define the stage of initiation of debonding, the slip distribution diagram (Fig. 15) and the load-slip diagram (Fig. 14) were considered simultaneously. For example, for specimens “L-EBR-1” and “L-EBR-2,” stages 30 and 60 were considered to be the initiation of the debonding stage. It can be observed that, after this stage, large slips occurred without the load increasing. From Figs. 14 and 15, it can be deduced that for the “L-EBROG-1” and “L-EBROG-2” stages 76 and 66 were the initiation of the debonding stage.

3.4.2. Prestressed FRP

Separation (r_f) of the central strip axis in Z direction during successive loading stages is exhibited in Fig. 16 for the release tests. In the prestress force-release tests, releasing the load was performed at $X = 0$ mm (called the loaded end in this study). Therefore, deformations were propagated from $X = 0$ mm to the unloaded end at $X = 300$ mm.

In the release specimens, the first eye-catching point is the very high separation values in the whole bond length compared to slips, which were experienced in the lap-shear tests. The bond behavior of prestressed FRP-to-concrete is, therefore, not a pure shear mode. In contrast, out-of-plane displacements play an important role, and mode II deformations governed the overall behavior of the prestressed FRP. While releasing the force, out-of-plane tensile stresses were engendered in the adhesive/concrete layer due to the eccentricity of the released force. These peeling stresses produced out-of-plane deformations.

It can be observed in Fig. 16 that, by using the EBROG method, much larger separations were generated in the substrate compared to that of the EBR method. EBR release tests reached to a maximum separation of 1.82 mm on average, while the corresponding separation of the EBROG release tests was 9.63 mm on average. It can be concluded that the EBROG method stiffened the concrete substrate to provide support for the bonded joint; thus, very high deformations were experienced, and high prestressing forces were carried by the bond.

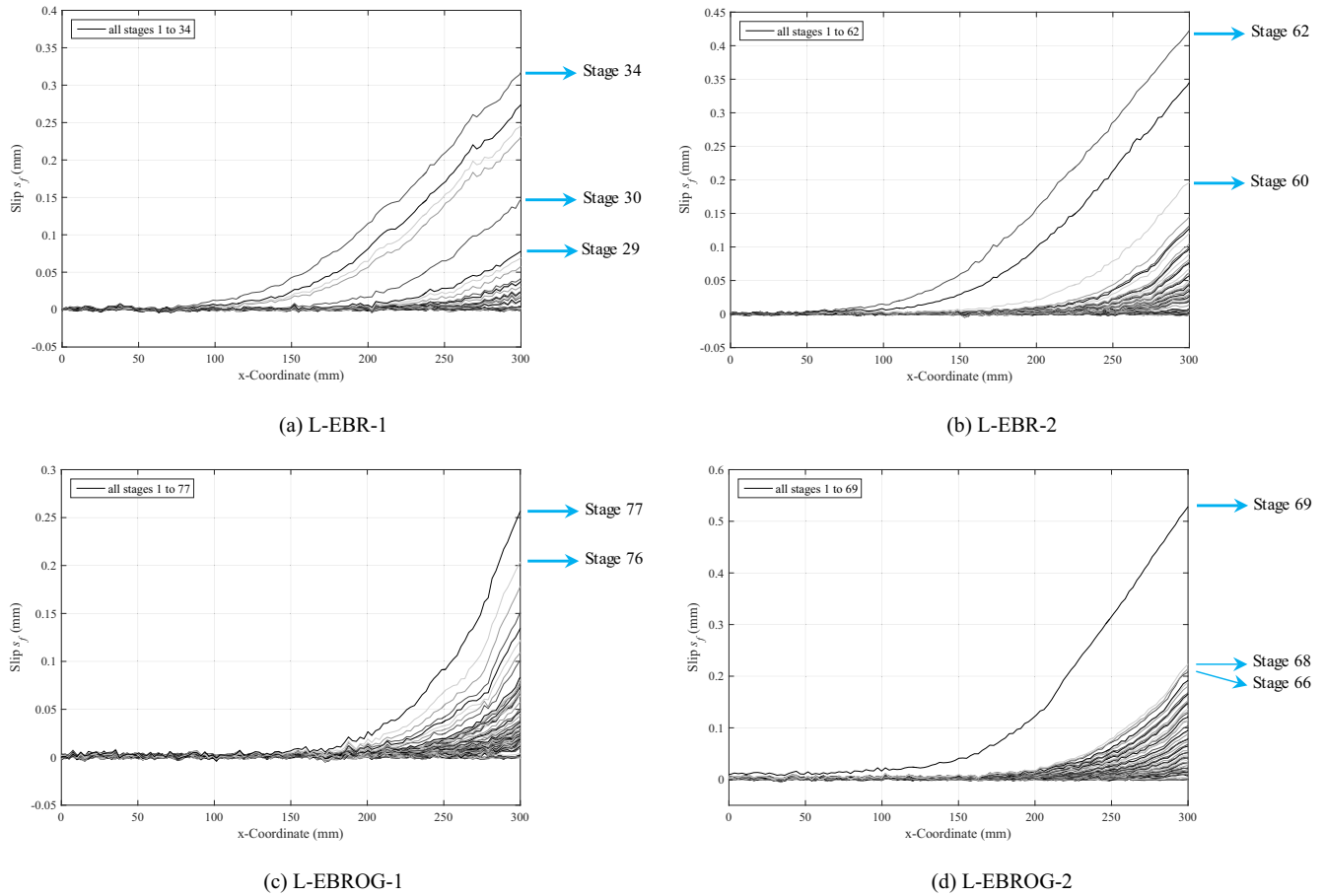


Fig. 15. Slip profiles in the bonded length of unstressed FRP, during the lap shear test.

From the failure mode (Fig. 12), it was observed that the debonded layer in the prestressed EBROG joints was under the grooves. In other words, the EBROG method transferred the stresses deep inside the concrete bulk. Besides, since the deep concrete was confined by the surrounding concrete, the cracks that developed in the concrete needed high energy and high force to be released. The releasing bond resistance of the EBROG method was, therefore, increased tremendously.

Similar clarification regarding the initiation of debonding was considered for release experiments by considering the separation profile evolutions instead of the slip profile evolutions. In the evolution of separation profiles of the EBR release specimens, several gaps were experienced (Fig. 16). For example, in specimen “R-EBR-1,” the separation profile that corresponded to the stage number 263, with a maximum separation of 0.299 at $X = 0$ mm, followed by a gap that indicated a significant increase in separation at the next stage. When comparing this stage with the load-separation diagram of the specimen, it can be seen that no increase in the force was experienced in this stage. Thus, debonding occurs at this stage, which is called the initiation of debonding in the release tests. A considerable increase in the affected bond length that experienced separation was also observed. Contrary to the lap shear tests, after this plateau in the load-slip curve of EBR specimens, a further increase in the load was achieved for the EBR release tests. This behavior is attributed to the tendency for crack propagation deep inside the concrete and the aggregate interlock,

which provided the ability of load increase. The behavior is, therefore, referred to as local debonding. After local debonding occurred, the separation profile is neither hyperbolic nor has a curvature in the first part; however, it has a straight line in the first debonded area. In contrast to the EBR release tests, the so-called local debonding with further load improvement was not experienced in the EBROG release experiments. Although there is a jump in slip profiles of specimen “R-EBROG-1,” no load increase was experienced afterward, and this stage was considered to be typical debonding. Specimen “R-EBROG-2” had similar typical debonding behavior to specimen “R-EBROG-1”.

3.5. Effective bond length for the unstressed FRP

Based on the well-known criteria, the effective bond length, l_{eff} , for the unstressed FRP strip is the active length at the stage of initiation of debonding. In the lap shear tests, the effective bond length was derived from the slip profile at the initiation of the debonding stage (Fig. 17). It can be observed that l_{eff} was approximately 155 mm for all EBR and EBROG lap shear joints. It is perceived that the effective bond lengths of the EBR and EBROG method, with the material properties that were used in this study, were almost equal, which means that the shear stress of EBROG was significantly higher (as the failure load was higher). However, it greatly depends on the concrete, FRP, and epoxy properties [31].

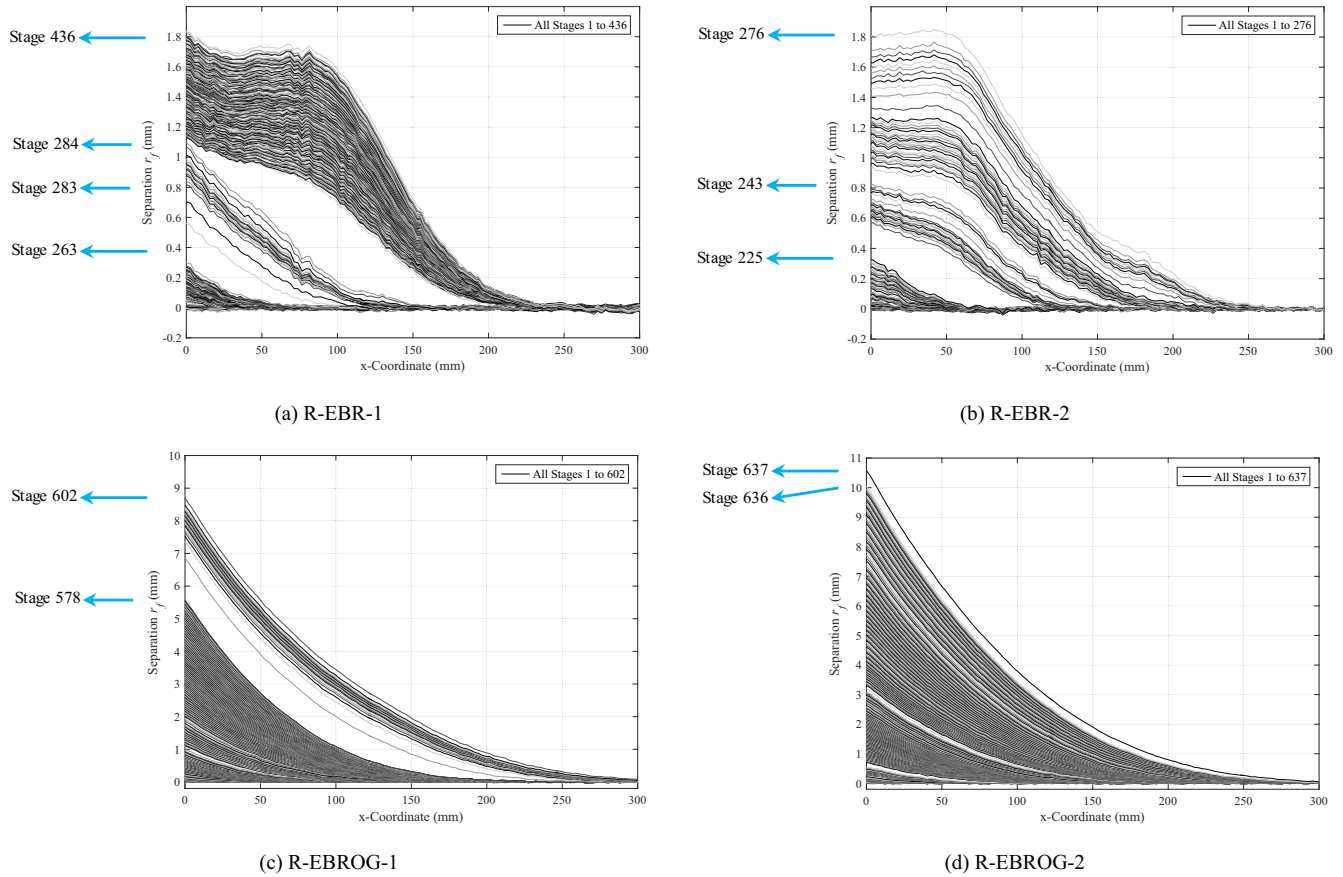


Fig. 16. Separation profiles in the bonded length of the prestressed FRP, during the release test.

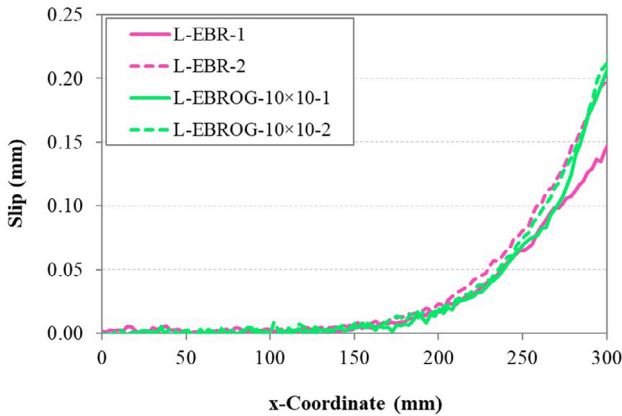


Fig. 17. Slip distribution at the initiation of debonding.

4. Conclusion

In the current study, the bond behavior of prestressed CFRP strips to concrete was inspected by conducting prestress force-release experiments and then was compared with the bond behavior of unstressed FRP strips in single-lap shear tests. Two different strengthening methods of EBR and EBROG were used to bond the strip to the concrete substrate. The recently introduced EBROG method was studied to improve the bond behavior of prestressed FRP-to-concrete for the first time. From the experiments, the following concluding remarks can be drawn:

1. Compared to the EBR method, the EBROG significantly increased the bond resistance of prestressed FRP-to-concrete. With the groove configuration used in this study, the bond resistance of the prestressed EBROG joints experienced a two-fold increase compared to that of the prestressed EBR joints. Prestressed EBR joints experienced bond resistances of 39.26 and 29.61 kN, while prestressed EBROG joints achieved bond resistances of 79.69 and 83.13 kN for the two repetitions.
2. The EBROG method provided a completely different path for crack growth in the concrete substrate, incorporating deep wide cracks beneath the prestressed CFRP strip. Therefore, the fracture energy increased and the bond resistance enhanced significantly.
3. Bond behavior of prestressed FRP to concrete entails large out-of-plane deformations, and thus cannot be treated as pure mode II behavior (shear mode). It is important to consider a mixed mode I/II behavior in future analytical/FE solutions.
4. The EBROG method resulted in higher out-of-plane deformations for prestressed FRP, compared to that of EBR, before failure because it resisted higher bond strengths.
5. The effective bond lengths were similar for unstressed EBR and EBROG specimens and equal to approximately 155 mm. However, it should be noted that the effective bond length might vary depending on groove configuration and material properties.

Considering the promising effect of the EBROG method on the bond behavior of prestressed FRP in addition to the unstressed strip, further investigation is suggested. In this regard, the effect of groove dimensions, material properties, and the prestressing level should be studied. Furthermore, flexural strengthening of

reinforced concrete beams with prestressed strips bonded by the EBROG method is of high interest and was studied by the authors, which will be published elsewhere.

CRedit authorship contribution statement

Niloufar Moshiri: Conceptualization, Methodology, Validation, Investigation, Formal analysis, Writing – original draft, Visualization, Funding acquisition. **Christoph Czaderski:** Methodology, Investigation, Validation, Supervision, Funding acquisition, Project administration. **Davood Mostofinejad:** Conceptualization, Methodology, Validation, Supervision. **Masoud Motavalli:** Validation, Project administration.

Declaration of Competing Interest

The authors declare that they have no known competing financial interests or personal relationships that could have appeared to influence the work reported in this paper.

Acknowledgments

The authors would like to sincerely thank the technicians at the Structural Engineering Research Laboratory of Empa. The first author was financed by the mobility grants received from Iran's Ministry of Science, Research and Technology (MSRT), Iran's National Elites Foundation, Empa Structural Engineering Research Laboratory, and ZHAW (Swiss Leading House for research collaboration with partner institutions) for the visiting research period at Empa. Also, financial support for performing the experiments and the materials used in this study were provided by S&P Clever Reinforcement Company AG, Switzerland, which is greatly acknowledged. This research was partly financed by the Iranian National Science Foundation (INSF) under project No. 96004203.

References

- [1] A. Tajmir-Riahi, N. Moshiri, D. Mostofinejad, Inquiry into bond behavior of CFRP sheets to concrete exposed to elevated temperatures–Experimental & analytical evaluation, *Compos. B Eng.* 173 (2019) 106897.
- [2] A. Tajmir-Riahi, N. Moshiri, C. Czaderski, D. Mostofinejad, Effect of the EBROG method on strip-to-concrete bond behavior, *Constr. Build. Mater.* 220 (2019) 701–711.
- [3] A. Tajmir-Riahi, N. Moshiri, D. Mostofinejad, EBROG method to strengthen heat-damaged concrete with CFRP sheets, SMAR 2019-Fifth conference on smart monitoring, assessment and rehabilitation of civil structures, Potsdam, Berlin, Germany, 2019.
- [4] R. El-Hacha, R.G. Wight, M.F. Green, Prestressed fibre-reinforced polymer laminates for strengthening structures: strengthening by prestressed FRP laminates, *Prog. Struct. Engng Mater.* 3 (2) (2001) 111–121.
- [5] R.G. Wight, M.F. Green, M.-A. Erki, Prestressed FRP sheets for poststrengthening reinforced concrete beams, *J. Compos. Constr.* 5 (4) (2001) 214–220.
- [6] S.-K. Woo, J.-W. Nam, J.-H. Kim, S.-H. Han, K.J. Byun, Suggestion of flexural capacity evaluation and prediction of prestressed CFRP strengthened design, *Eng. Struct.* 30 (12) (2008) 3751–3763.
- [7] W. Xue, Y. Tan, L. Zeng, Flexural response predictions of reinforced concrete beams strengthened with prestressed CFRP plates, *Compos. Struct.* 92 (3) (2010) 612–622.
- [8] M. Motavalli, C. Czaderski, K. Pfl-Lang, Prestressed CFRP for strengthening of reinforced concrete structures: Recent developments at Empa, Switzerland, *Journal of Composites for Construction* 15 (2) (2010) 194–205.
- [9] N. Moshiri, C. Czaderski, D. Mostofinejad, A. Hosseini, K. Sanginabadi, M. Breveglieri, M. Motavalli, Flexural strengthening of RC slabs with nonprestressed and prestressed CFRP strips using EBROG method, *Compos. B Eng.* 201 (2020) 108359.
- [10] P. Fernandes, J. Sena-Cruz, C. Fernandes, P. Silva, D.D.d. Costa, E. Júlio, Flexural response of HSC girders strengthened with non-and prestressed CFRP laminates, FRPRCS-11: 11th International Symposium on Fiber Reinforced Polymer for Reinforced Concrete Structures, Universidade do Minho, 2013.
- [11] C. Pellegrino, C. Modena, Flexural strengthening of real-scale RC and PRC beams with end-anchored pretensioned FRP laminates, *ACI Struct. J.* 106 (3) (2009) 319–328.
- [12] D.-S. Yang, S.-K. Park, K.W. Neale, Flexural behaviour of reinforced concrete beams strengthened with prestressed carbon composites, *Compos. Struct.* 88 (4) (2009) 497–508.
- [13] T. Siwowski, B. Piątek, P. Siwowska, A. Wiater, Development and implementation of CFRP post-tensioning system for bridge strengthening, *Eng. Struct.* 207 (2020) 110266.
- [14] Y.-C. You, K.-S. Choi, J. Kim, An experimental investigation on flexural behavior of RC beams strengthened with prestressed CFRP strips using a durable anchorage system, *Compos. B Eng.* 43 (8) (2012) 3026–3036.
- [15] R. El-Hacha, R.G. Wight, M.F. Green, Prestressed Carbon Fiber Reinforced Polymer Sheets for Strengthening Concrete Beams at Room and Low Temperatures, *J. Compos. Constr.* 8 (1) (2004) 3–13.
- [16] C. Czaderski, Strengthening of reinforced concrete members by prestressed externally bonded reinforcement with gradient method, Ph.D. Thesis, ETH Zürich, Zürich, Switzerland (2012), <https://doi.org/10.3929/ethz-a-007569614>.
- [17] J. Michels, E. Zile, C. Czaderski, M. Motavalli, Debonding failure mechanisms in prestressed CFRP/epoxy/concrete connections, *Eng. Fract. Mech.* 132 (2014) 16–37.
- [18] C. Czaderski, M. Motavalli, 40-Year-old full-scale concrete bridge girder strengthened with prestressed CFRP plates anchored using gradient method, *Compos. B Eng.* 38 (7) (2007) 878–886.
- [19] J. Michels, J. Sena-Cruz, C. Czaderski, M. Motavalli, Structural strengthening with prestressed CFRP strips with gradient anchorage, *J. Compos. Constr.* 17 (5) (2013) 651–661.
- [20] W. He, X. Wang, Z. Wu, Flexural behavior of RC beams strengthened with prestressed and non-prestressed FRP grids, *Compos. Struct.* 246 (2020) 112381.
- [21] B.N. Tehrani, D. Mostofinejad, S.M. Hosseini, Experimental and analytical study on flexural strengthening of RC beams via prestressed EBROG CFRP plates, *Eng. Struct.* 197 (2019) 109395.
- [22] D. Mostofinejad, E. Mahmoudabadi, Grooving as Alternative Method of Surface Preparation to Postpone Debonding of FRP Laminates in Concrete Beams, *J. Compos. Constr.* 14 (6) (2010) 804–811.
- [23] D. Mostofinejad, S.M. Shamel, Externally bonded reinforcement in grooves (EBRIG) technique to postpone debonding of FRP sheets in strengthened concrete beams, *Constr. Build. Mater.* 38 (2013) 751–758.
- [24] N. Moshiri, A. Hosseini, D. Mostofinejad, Strengthening of RC columns by longitudinal CFRP sheets: Effect of strengthening technique, *Constr. Build. Mater.* 79 (2015) 318–325.
- [25] D. Mostofinejad, N. Moshiri, Compressive Strength of CFRP Composites Used for Strengthening of RC Columns: Comparative Evaluation of EBR and Grooving Methods, *J. Compos. Constr.* 19 (5) (2015) 04014079.
- [26] D. Mostofinejad, M. Hajirasouliha, Shear Retrofitting of Corner 3D-Reinforced Concrete Beam-Column Joints Using Externally Bonded CFRP Reinforcement on Grooves, *J. Compos. Constr.* 22 (5) (2018) 04018037.
- [27] A. Torabian, D. Mostofinejad, Externally bonded reinforcement on grooves technique in circular reinforced columns strengthened with longitudinal carbon fiber-reinforced polymer under eccentric loading, *ACI Struct. J.* 114 (4) (2017) 861–873.
- [28] D. Mostofinejad, M. Heydari Mofrad, A. Hosseini, H. Heydari Mofrad, Investigating the effects of concrete compressive strength, CFRP thickness and groove depth on CFRP-concrete bond strength of EBROG joints, *Constr. Build. Mater.* 189 (2018) 323–337.
- [29] A. Hosseini, D. Mostofinejad, Effect of groove characteristics on CFRP-to-concrete bond behavior of EBROG joints: Experimental study using particle image velocimetry (PIV), *Constr. Build. Mater.* 49 (2013) 364–373.
- [30] A. Hosseini, D. Mostofinejad, Experimental investigation into bond behavior of CFRP sheets attached to concrete using EBR and EBROG techniques, *Compos. B Eng.* 51 (2013) 130–139.
- [31] N. Moshiri, A. Tajmir-Riahi, D. Mostofinejad, C. Czaderski, M. Motavalli, Experimental and analytical study on CFRP strips-to-concrete bonded joints using EBROG method, *Compos. B Eng.* 158 (2019) 437–447.
- [32] A. Tajmir-Riahi, N. Moshiri, D. Mostofinejad, Bond mechanism of EBROG method using a single groove to attach CFRP sheets on concrete, *Constr. Build. Mater.* 197 (2019) 693–704.
- [33] M.S. Salimian, D. Mostofinejad, Experimental Evaluation of CFRP-Concrete Bond Behavior under High Loading Rates Using Particle Image Velocimetry Method, *J. Compos. Constr.* 23 (3) (2019) 04019010, [https://doi.org/10.1061/\(ASCE\)CC.1943-5614.0000933](https://doi.org/10.1061/(ASCE)CC.1943-5614.0000933).
- [34] A. Tajmir-Riahi, D. Mostofinejad, N. Moshiri, Bond resistance of a single groove in EBROG method to attach CFRP sheets on concrete, Proceedings of the ninth international conference on fibre-reinforced polymer (FRP) composites in civil engineering (CICE 2018), Paris, France, 2018, pp. 368–373.
- [35] N. Moshiri, D. Mostofinejad, A. Tajmir-Riahi, Bond behavior of pre-cured CFRP strips to concrete using externally bonded reinforcement on groove (EBROG) method, Proceedings of the ninth international conference on fibre-reinforced polymer (FRP) composites in civil engineering (CICE 2018), Paris, France, 2018, pp. 361–367.
- [36] D. Mostofinejad, A.T. Kashani, Experimental study on effect of EBR and EBROG methods on debonding of FRP sheets used for shear strengthening of RC beams, *Compos. B Eng.* 45 (1) (2013) 1704–1713.
- [37] C. Czaderski, N. Moshiri, A. Hosseini, D. Mostofinejad, M. Motavalli, EBROG technique to enhance the bond performance of CFRP strips to concrete substrate, SMAR 2019-Fifth conference on Smart Monitoring, assessment and rehabilitation of civil structures, Potsdam-Berlin, Germany, 27–29 August 2019.

- [38] N. Moshiri, C. Czaderski, D. Mostofinejad, M. Motavalli, Bond strength of prestressed CFRP strips to concrete substrate: comparative evaluation of EBR and EBROG methods SMAR 2019-Fifth conference on Smart Monitoring, assessment and rehabilitation of civil structures, Potsdam-Berlin, Germany,, 27-29 August 2019.
- [39] S&P Clever Reinforcement, Technical data sheet, S&P CFRP-laminates, carbon fiber plates for structural reinforcement, <https://www.sp-reinforcement.ch/de-CH>, S&P Clever Reinforcement Company AG, CH-6423 Seewen, Switzerland, 2015.
- [40] A. Hosseini, E. Ghafoori, M. Wellauer, A. Sadeghi Marzaleh, M. Motavalli, Short-term bond behavior and debonding capacity of prestressed CFRP composites to steel substrate, *Eng. Struct.* 176 (2018) 935–947.
- [41] ARAMIS - User Manual Software v. 6.3. GOM GmbH Braunschweig, Germany, , 2008.